Article:

Srinivasan, AR orcid.org/0000-0001-9280-7837, Karan, FSN and Chakraborty, S (2017) Pedestrian dynamics with explicit sharing of exit choice during egress through a long corridor. Physica A: Statistical Mechanics and its Applications, 468. pp. 770-782. ISSN 0378-4371

https://doi.org/10.1016/j.physa.2016.11.118

Pedestrian dynamics with explicit sharing of exit choice during egress through a long corridor

Aravinda Ramakrishnan Srinivasan, Farshad Salimi Naneh Karan
and Subhadeep Chakraborty*

Mechanical, Aerospace and Biomedical Engineering Department, University of Tennessee, Knoxville, 1512 Middle Dr, Knoxville, TN 37996 , USA

Abstract

The egress literature abounds with studies and models of emergency pedestrian evacuation behavior. Each model tries to incorporate more details and features of the crowd movement dynamics to improve its accuracy. This paper combines a relatively simple pedestrian motion model with a position dependent Voter model to study the effects of opinion sharing on crowd evacuation characteristics. Effect of the presence of leaders on the final outcome of the evacuation is studied in detail. An analytical solution for a simplified version of the egress dynamics with opinion exchange is presented, followed by a set of numerical simulations. Interesting findings about the effect of the strength of interaction between individuals, number and distribution of leaders and initial bias of the evacuees on the final distribution of evacuees over available exits, mean number of steps to evacuate, etc. are presented.

Keywords: Egress modeling, Hybrid model - motion and opinion sharing model, Analytical solution, Effect of leaders

1. Introduction

The planning authorities take into account various factors when deciding on a particular evacuation procedure for each building in case of an emergency. Factors like

*Corresponding author
Email address: asriniv2@vols.utk.edu,~fsalimin@vols.utk.edu and~schakrab@utk.edu (Aravinda Ramakrishnan Srinivasan, Farshad Salimi Naneh Karan and Subhadeep Chakraborty)

maximum capacity of an exit, maximum allowed occupancy of the building, minimum time to evacuate, etc. play important roles in this planning. Researchers have tried to model the evacuation procedure to study the various parameters involved and to optimize the evacuation plan. Several existing emergency evacuation simulators try to take into account as many factors as possible to effectively calculate the time to evacuate and also test the efficacy of different evacuation procedures or to compute an optimized plan for egress. However, a careful look at the state-of-the-art in egress literature shows that although tremendous progress has been made in modeling pedestrian movement in emergency, the effect of 'herding' tendencies on egress dynamics has not received as much attention. This paper starts with a simple egress situation but incorporates the effect of group interaction on route choice and hence the movement dynamics of individuals. The movement dynamics in turn affects the instantaneous formation and dissipation of small groups of evacuees. To the best of our knowledge, these two complementary dynamics (decision and movement) has not been analytically and numerically investigated in the context of egress in the past.

1.1. Literature Review

A comprehensive literature review of the state-of-the-art in egress research is provided here to motivate the research carried out in this paper and also to serve as a quick resource for researchers in the field.

1.1.1. Fluid Flow Models

Hughes et.al. [1, 2, 3] modeled the movement of pedestrians as fluid flow by identifying the governing equations for the fluid flow model. This work identifies the human crowd as analogous to thinking fluids and studies the effect of barrier placement to improve the flow of the crowd. Colombo et.al. [4] studied the effect of panic with the continuum fluid flow model. These models, though conforming largely with experimental data fails to take into account the role of interactions among egressing individuals in determining their exit choices and overall movement dynamics.

1.1.2. Cellular Automata Models

Cellular automata principles have been used to model the pedestrian flow in [5]. In [6], Helbing used velocity equations for individuals and incorporates personal preferences and environmental effects to model the movement of pedestrians, while in [7], deceleration and other changes in velocity were utilized to account for others in pedestrian movement. However, the exit choice is fixed. Burstedde et.al. [8] used a $2D$ cellular automaton to model the pedestrian dynamics. Using a method similar to potential field, he studied the model's statistical properties using Monte Carlo simulations. The individual interactions are not explicit but implicit through the usage of floor field. Using a similar cellular automaton along with potential field method, Varas et.al. [9] discussed the merits of door size, position of door relative to obstacles in the room and their effects on the time to evacuate. The model was used to study the evacuation from a classroom at full capacity. Seitz et.al. [10] studied leader-follower behavior with loss of line of sight of leader and subsequent decision making. This is a movement model that incorporates leaders but the interaction between leader and follower is fixed and pre-determined. Though these models have their unique way of representing the motion of individuals, there is scope to improve the decision mechanism that supports the motion model.

Kirchner et.al. [11, 12] tried to model the movement of people in emergency evacuation using the principles of cellular automata and the social force model developed by Helbing et. al.[6]. In this work, the building was divided into discrete cells and the interplay between two force fields was studied - a static field to account for factors like the desired exit, obstacles in the way and a dynamic field to take into account the effect of other nodes/people. A model with static field and a friction coefficient to control the competitive behavior was presented in [11] and it matches experimental data from an airplane evacuation. In [12], the effect of others is indirectly taken into account through the traces they leave on the path followed (dynamic field). Kirchner et.al. [13] studied the effect of various cell sizes and different maximum velocities on the model. Kluepfel [14] presented a complete study of how different velocities of individuals can be computed taking into account various factor like age, gender, etc. and modeled the competition between people as analogous to Newtonian friction. Henein et.al. [15] took the work of Kirchner et.al., added another field that takes into account the force interaction between individuals and simulated injuries due to force interaction and its effect on the evacuation time. This model is one more step toward adding all relevant interactions that takes place during evacuation. Nevertheless, in all these studies, the individual route choice is predetermined and effect of interaction among individuals on the exit choice is not taken into account.

Parisi et.al. [16] used the social force model to study the effect of different degrees of panic. The different degrees of panic is simulated through different desired individual's velocity. It is described as 'faster is slower' effect in [6]. The effect of door sizes with different panic level on the evacuation time is studied in detail. The panic level is found to affect the formation of clusters among the nodes and the distribution of cluster mass/size is found to have to a 'U' shaped characteristic curve with the panic level/desired velocity [17]. Again, this model gives a comprehensive simulation for only the movement dynamics of evacuation.

1.1.3. Lattice Model

Lattice gas models have been used to model and verify a classroom evacuation in [18]. The particles in the simulation execute a biased random walk toward the exit and the model takes into account personal space/minimum distance to avoid collision as well as obstacles, but in this work, the exit choice was pre-determined and lacked an explicit model for route choices. Takimoto et.al. [19] used the lattice gas model of pedestrian movement to study the relationship between escape time through an exit and the starting position of people in the room. Additionally, the effect of exit width on the distribution of escape time was also examined. Song et.al and Guo et.al. [20, 21] combined the lattice gas model with the social force model and thus tried to incorporate interaction among individuals implicitly through the force fields. The average evacuation time found using simulations combining both models were found to be more accurate compared to the lattice gas model alone. This further strengthens the need for a decision making model that more explicitly takes into account exit choice as well as one-on-one and group interactions.

1.1.4. Discrete Event Model and Game Theoretic Model

Lino et.al. [22] modeled the crowd egress dynamics with the principles of queueing in networks. Singh et.al. [23] utilized a discrete event model. The effect of leaders and sub groups in crowd dynamics was examined in detail, but still does not involve inter personal opinion sharing to support the excellent movement model. Lo et.al. [24] used a game theoretic approach to model the exit choice of individual. A virtual agent played against each individual(s) till Nash equilibrium was arrived for each step to decide on the exit choice of the individual(s). This also falls into category of implicit decision/opinion sharing. Work has been done to model and simulate a crowd guidance mechanism to help the crowd to safety in shortest possible time. Gao et.al. [25] take into account the confidence level of individuals in either accepting or rejecting guidance. Wang et.al. [26] tried to build an intelligent crowd guidance system by giving a probability of accepting of the guidance. Directed graphs and Markov Decision Processes were used to solve the optimization with respect to avoiding blocking of pathway. This work also incorporated model for fire propagation and crowd impatience in the optimization. These works highlight the importance for a guidance system to help optimize the evacuation time.

1.1.5. Psychological Model

Proulx [27] stresses the need for better understanding of human interaction under emergency. Hasan et.al. [28] examined the effect of person's social network on their decision to evacuate on receiving a hurricane warning. It was found that individuals' social links and the amount of trust they have on their links strongly influences their decision to evacuate. Goldstone et.al. [29] used agent based modeling to study the group behavior from a psychology point of view but this lacks the complementary motion model to become a complete egress model. Spieser et.al. [30, 31, 32, 33] studied just the psychological dynamics in opinion control. Using Gustav LeBon's suggestibility theory [34], a collective behavior model was utilized for developing a discrete-time non linear model of crowd psychological behavior. The elements of a queue were agitated and a control algorithm to bring the agitated elements to normal state using one or more control node(s) was derived. Though the psychological aspect is well modeled, lack of a motion model limits its utility as a complete egress model. On other hand, Pan et.al. [35, 36, 37, 38] attempted to build a simulation system that takes social interaction among individual nodes through simulated perception of current environment and a set of rules/decision tree to come up with a valid action for each set of sensed input. This work combines both motion and interaction model albeit the interaction among crowd is still implicit and there is no direct interaction/sharing of exit choice opinion among the nodes. Kuligowski and Zheng et.al. [39, 40] gave comprehensive overview of existing egress simulation techniques.

As evident from the literature reviewed above, there is a need for a model that combines the two coupled aspects of egress - a motion model and also an explicit opinion sharing framework between the exiting individuals. In an emergency, a group will make their choices of different escape routes by taking into account not only their individual predispositions, distances to exits, familiarity with the environment, obstacles in their path, perceived sense of danger, etc., but also through imitation of and influence from people who are physically nearby. It is also possible that a few amongst the crowd will display a strong attraction towards one of the exit choices available, borne out of prior knowledge of the environment or their natural predisposition to be leaders or confident in their decision making. The effect of strong opinion holders on the egress dynamics poses an interesting problem.

This work studies a simplified model of movement along with an opinion sharing framework to study the combined effect of both.

2. Modeling of crowd movement dynamics with opinion sharing

For the purpose of this paper, a long corridor with two exits (an exit to left (E_L) and an exit to right (E_R)) is considered. At each instant, each individual of the crowd can choose to use either of the two exits and correspondingly, move one step toward right or left end exit of the corridor. To account for the explicit swapping of exit choice information among individuals, the voter model dynamics is utilized. According to this dynamics, at arbitrary time steps, one random individual is spontaneously influenced by one of his physically close neighbors, chosen at random. If the neighbor happens

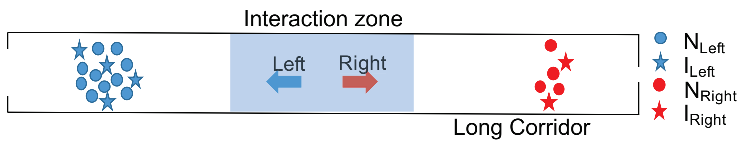

Figure 1: Illustration of a long narrow corridor with a group moving toward either side

to be moving in the same direction as him, he finds reinforcement in his belief that he is indeed going in the optimal (safest) direction. If the neighbor happens to be rushing towards the other exit, that introduces doubt and leads to him changing his decision. Plausibly, this influence is modeled to get weaker as the individual and his neighbor are further away from each other. In the analytical model, all individuals are assumed to start at the center of the corridor and an interaction zone starting at the center of the corridor and stretching to 20% of the total length of the corridor on either side is established. The individuals can successfully affect other's exit decision only if both are within the interaction zone. To account for the motion model, after every decision step, every individual of the crowd moves one step towards their respective exit choice. However, if an individual changes his/her exit choice they are assumed to be able to join up with the new group instantaneously. The rationale behind this assumption is borrowed from considering the crowd movement as a choked fluid flow through a narrow bottleneck, where people move much slower as a group due to crowding in a narrow space. Consequently, the passage between the two groups is largely empty and the individuals switching between groups can join their new group relatively quickly. To study this motion with opinion model analytically, a Master equation approach, developed previously in [41, 42] is utilized. For completeness and clarity, the master equation and a polynomial solution is derived below.

2.1. Analytical Solution

Let, at a given instant, the number of people without strong opinions moving toward E_R be denoted by N_R and the number moving toward E_L be denoted by N_L. The total number of indecisive people moving is thus $N = N_R + N_L$. In addition, there are I_R people strongly predisposed to move toward the right exit while I_L having a strong bias toward the left exit, for a total of $I = I_R + I_L$ evacuees with strong opinions. This is illustrated in Fig. 1

Let us now define three variables - the crowd polarization parameter, $p = \frac{N_R - N_L}{N}$, the influencer ratio, $u = \frac{I_R - I_L}{I}$ and the global influence ratio, $\zeta = \frac{I}{N}$. The crowd polarization parameter $p \in [-1, 1]$ captures the ratio of people moving right vs. moving left. Thus, $p = 1$ means that everybody is moving towards the right exit at that instant, $p = -1$ means that everybody is moving towards the left exit at that instant and $p = 0$ means that half are moving towards right and the rest toward left. The influencer ratio, u denotes the relative influence or control that people with strong opinions, (who we will subsequently identify as 'leaders') have over the independent decision makers' possible exit choices. $u = \pm 1$ denotes each of the independent thinkers are moving towards the exit on the right side (or left side) of the long corridor, $u = 0$ indicates that there is equal number of leaders attracting the crowd towards both the exits. The global influence ratio, ζ is the fraction of the number of influencers to the number of indecisive people. $\zeta = 0$ implies there are no influencers in the crowd. As ζ increases, the number of strong opinion holders in the crowd increases until at $\zeta = 1$ the whole crowd comprises individuals holding strong opinions. The master equation for this stochastic system is given by

$$\dot{P}_p = r_{p+\frac{2}{N}} P_{p+\frac{2}{N}} + g_{p-\frac{2}{N}} P_{p-\frac{2}{N}} - (r_p + g_p) P_p \tag{1}$$

where,

$$\begin{aligned}
r_p = P(p \to p - \frac{2}{N}) &= \left(\frac{N_R}{N}\right)\left(\frac{N_L + I_L}{N + I - 1}\right) \\
g_p = P(p \to p + \frac{2}{N}) &= \left(\frac{N_L}{N}\right)\left(\frac{N_R + I_R}{N + I - 1}\right) \\
r_{p+\frac{2}{N}} &= \left(\frac{N_R + 1}{N}\right)\left(\frac{N_L - 1 + I_L}{N + I - 1}\right) \\
g_{p-\frac{2}{N}} &= \left(\frac{N_L + 1}{N}\right)\left(\frac{N_R - 1 + I_R}{N + I - 1}\right)
\end{aligned} \tag{2}$$

Substituting Eqn. 2 in Eqn. 1, we get

$$\begin{aligned}\dot{P}_p = \left(\frac{N_R+1}{N}\right)\left(\frac{N_L-1+I_L}{N+I-1}\right)P_{p+\frac{2}{N}} \\ +\left(\frac{N_L+1}{N}\right)\left(\frac{N_R-1+I_R}{N+I-1}\right)P_{p-\frac{2}{N}} \\ -\left[\left(\frac{N_R}{N}\right)\left(\frac{N_L+I_L}{N+I-1}\right)+\left(\frac{N_L}{N}\right)\left(\frac{N_L+I_L}{N+I-1}\right)\right]P_p\end{aligned} \tag{3}$$

For large N, assuming that $I < N$, $I_L P_{p+2/N} + I_R P_{p-2/N} \approx I P_p$, with proper scaling of time as $\tau = t/N^2$ and noting that $N_R I_L - N_L I_R = \frac{NI}{2}(p-i)$, the master equation can be simplified [41] to its final form as,

$$\frac{\partial P_p}{\partial \tau} = \frac{1}{2}\frac{\partial^2}{\partial p^2}\left[B(p)P_p\right] - \frac{\partial}{\partial p}\left[A(p)P_p\right] \tag{4}$$

$$\text{where,} \quad B(p) = 2\left(1-p^2\right) \tag{5}$$

$$A(p) = I\left(u-p\right) \tag{6}$$

Equation 4 describing the time evolution of the probability density function of the polarization parameter p, can be recognized as the Fokker-Planck equation and can be treated with generic methods developed for such partial differential equations. Wong et.al. [43] has reported certain general conditions under which the problem reduces to an eigenvalue problem of the Sturm-Liouville type and gives rise to polynomial solutions. If it is assumed that an equilibrium density function exists, and

$$\lim_{\tau\to\infty}\frac{\partial P_p}{\partial \tau} = 0 \tag{7}$$

then it is simple to show that the equilibrium density $p_e(m)$ satisfies

$$\frac{d}{dp}\left((1-p^2)p_e(p)\right) - I(u-p)p_e(p) = 0 \tag{8}$$

if the constants of integration are assumed to be 0. Substituting $P_p(\tau) = f(\tau)p_e(p)\varphi(p)$, in Eqn. 4 and using separation of variables,

$$\frac{df(\tau)}{d\tau} = -\lambda f(\tau) \tag{9}$$

$$\frac{d^2}{dp^2}\left((1-p^2)p_e(p)\varphi(p)\right) - \frac{d}{dp}\left(I(u-p)p_e(p)\varphi(p)\right) = -\lambda p_e(p)\varphi(p) \tag{10}$$

Assuming discrete eigenvalues, Eqn. 9 can be easily solved to yield,

$$f_n(\tau) = k_n e^{-\lambda_n \tau} \tag{11}$$

while using Eqn. 8 in Eqn. 10 gives the Sturm-Liouville form,

$$\frac{d}{dp}\left((1-p^2)p_e(p)\frac{d\varphi(p)}{dp}\right) + \lambda p_e(p)\varphi(p) = 0 \tag{12}$$

Necessary and sufficient conditions for Eqn. 12 to yield a complete orthonormal set of polynomials as eigenfunctions have been studied by Wong et. al. [43]. They can be summarized as follows:

$$B(p_1)p_e(p_1) = B(p_2)p_e(p_2) = 0, \tag{13}$$

$$\text{where} \quad p_1 \leq p \leq p_2$$

$$A(p) = ap + b \tag{14}$$

$$B(p) = cp^2 + dp + e \quad \text{and} \tag{15}$$

$$\int_{p_1}^{p_2} p^n p_e(p)dp < \infty, \quad n = 0, 1, ..., n < \infty \tag{16}$$

From Eqn. 5,6 and noting that $-1 \leq p \leq 1$, it is easy to see that the necessary and sufficient conditions are satisfied. The above conditions restrict the density function $p_e(p)$ to be of the form [43],

$$p_e(p) = \frac{1}{2^{\alpha+\beta+1}}\frac{\Gamma(\alpha+\beta+2)}{\Gamma(\alpha+1)\Gamma(\beta+1)}(1-p)^{\alpha}(1+p)^{\beta}, \quad \alpha, \beta > -1 \tag{17}$$

while the polynomial eigenfunctions $\varphi_n(p)$ orthonormalized with respect to the equilibrium density function $p_e(p)$ are the Jacobi polynomials,

$$\begin{aligned} \varphi_n(p) = {} & \frac{(-1)^n}{2^n} \times \sqrt{\frac{(2n+\alpha+\beta+1)\Gamma(n+\alpha+\beta+1)}{\Gamma(n+\alpha+1)\Gamma(n+\beta+1)}} \\ & \times \sqrt{\frac{\Gamma(\alpha+1)\Gamma(\beta+1)}{\Gamma(\alpha+\beta+2)n!}} \times (1-p)^{-\alpha}(1+p)^{-\beta} \\ & \times \frac{d^n}{dp^n}\left[(1-p)^{n+\alpha}(1+p)^{n+\beta}\right] \end{aligned} \tag{18}$$

For $p_e(p)$ defined as in Eqn. 17, the functions

$$\begin{aligned} A(p) &= \gamma(\beta-\alpha) - \gamma(\alpha+\beta+2)p \\ &= Iu - Ip \qquad \text{(from Eqn.6)} \\ B(p) &= 2\gamma(1-p^2) \\ &= 2(1-p^2) \qquad \text{(from Eqn.5)} \\ \text{and} \quad \lambda_n &= \gamma n(n+\alpha+\beta+1) \end{aligned} \tag{19}$$

Solving 19 yields

$$\begin{aligned} \gamma &= 1, \\ \lambda_n &= n(n+I-1), \\ \alpha &= I_L - 1 \text{ and} \\ \beta &= I_R - 1 \end{aligned} \tag{20}$$

This restricts $I_R, I_L \geq 1$. The joint probability density function $p(p_0, p; \tau)$ have the form,

$$p(p_0, p; \tau) = p_e(p_0)p_e(p) \sum_{n=0}^{\infty} e^{-\lambda_n \tau} \varphi_n(p_0)\varphi_n(p) \tag{21}$$

where p_e, φ_n and λ_n are given by respectively Eqns. 17, 18 and 19, and initial polarization factor $p_0 = p(\tau_0)$. This completely specifies the progression of the joint probability density function.

The results shown in Fig. 2 are for $N = 200$, $p_0 = 0$, $I_R = 11$ and $I_L = 2$. In other words, initially exactly 50% of the 200 undecided evacuees start moving right and 50% start towards the left exit. As they start moving as two discrete groups, there is opinion exchange and a few people change their mind and join the other group moving in the opposite direction. Figure 2 shows the probability distribution of how the crowd is expected to be polarized at each subsequent time steps. Numerical results from 2500 Monte Carlo simulations overlayed on the analytical results verify the accuracy of the results and the validity of the assumptions made. Interestingly, with increasing number of average interactions per person, the probability distribution flattens out, while the mean slowly moves towards higher values of p. The gradual favoring of the right exit by more people is a result of the larger number of independent nodes moving to the right ($I_R = 11$) compared to the left ($I_L = 2$).

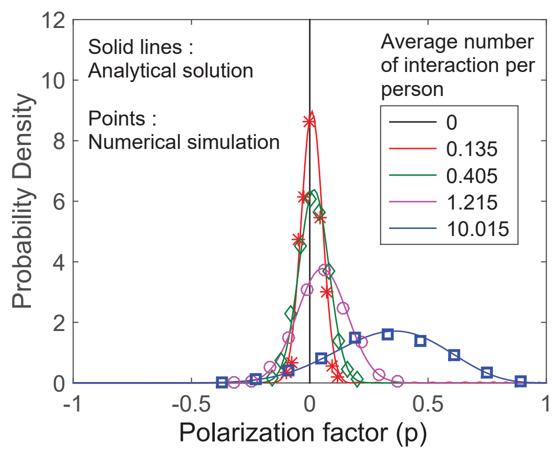

Figure 2: Analytical and numerical results for probability distribution of final crowd polarization factor with different number of average interaction per person. Here, $N = 200$, $p_0 = 0$, $I_R = 11$ and $I_L = 2$.

From the point of view of faster evacuation, it is beneficial to be able to influence the final polarization to match the flow capacity of the individual exits. For example, in our experiments, if the right exit has twice the flow capacity of the left exit, then it is preferred that the crowd polarization (p) is equal to 0.33. The analytical and numerical results suggest that the the presence of strong opinion holders has an enormous effect on polarizing the crowd, thereby affecting the total evacuation time by utilizing the available exits more or less effectively.

2.2. Constant velocity dynamics

In the previous section, movement of individuals from one group to another is assumed to occur at a faster time scale compared to the group movement. This dynamics was modeled on the assumption that individuals move faster than a tightly packed crowd trying to navigate a narrow corridor. But this assumption fails to hold if we consider a larger space where individuals are free to move at their own pace, limited only by their physical capabilities. In that scenario, formation of distinct clusters of people moving together is unlikely, rather a more uniformly spread out distribution over the movement axis seems to be more probable. To investigate the implications of this scenario, a constant velocity model is investigated next. Each node, i is assumed

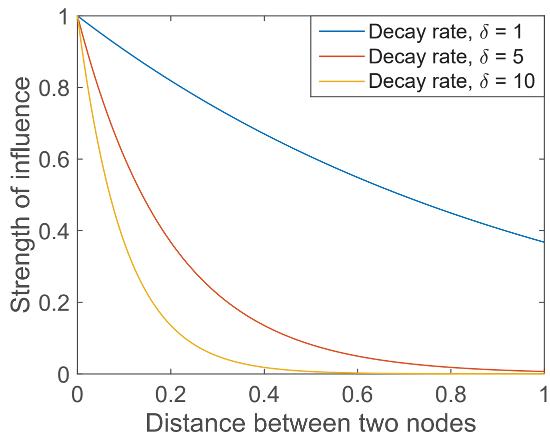

Figure 3: Strength of influence between two nodes with different decay rates (δ)

to be moving at their maximum speed toward their respective choice of exit, σ_i, where $\sigma_i \in \{E_L, E_R\}, \forall i \in N \cup I$. Unlike the previous case, the strength of interaction between two individuals is now modeled as a function of the distance separating them. In this case, we model the strength of interaction as $SOI(d_{ij}) = e^{-\delta \times d_{ij}}$, where δ is the decay rate and d_{ij} is the distance between nodes i and j at that instant. Incorporating the SOI factor, the modified Voter model dynamics is now as follows (Alg. 1).

Essentially, for a higher decay rate, the interaction is similar to that implemented with the previously discussed narrow central interaction zone, inside which all interactions are constrained to occur. For lower decay rates, even more distant individuals have a higher probability of successfully changing the opinion of the other. This strength of interaction creates a personal interaction zone for each individual separately and it moves with the individual. The size of the interaction zone is determined by the decay rate.

Leaders are recognized by their ability to influence a large number of people. This is modeled by relaxing the distance restriction on the SOI for such individuals, i.e., leaders are assumed to be able to influence undecided individuals successfully, regardless of the distance between them. With this setup various numerical simulation experiments were carried out and the results are presented and discussed in the following section.

Algorithm 1: Hybrid motion model with strength of influence voter model

Data: N, I_R, I_L, δ

Result: Decision sharing model with SOI

Initialization: $p_0, \{\sigma_i : i \in N \cup I\}$;

while *egress is not complete* **do**

  while *each node hasn't interacted once* **do**

    Select each node i in random order, where $i \in N$;

    Select random neighbor j for each, where $j \in N \cup I$;

    Determine $SOI(d_{ij}) = e^{-\delta \times d_{ij}}$;

    Set $\sigma_i = \sigma_j$ with probability $SOI(d_{ij})$;

  end

  Each node i moves one step towards their exit choice σ_i, where $i \in N \cup I$

end

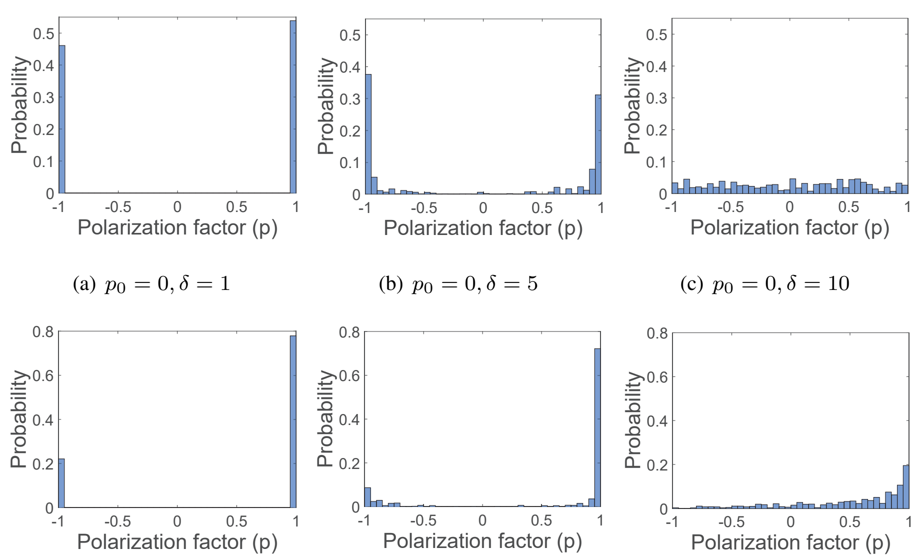

(a) $p_0 = 0, \delta = 1$ (b) $p_0 = 0, \delta = 5$ (c) $p_0 = 0, \delta = 10$

(d) $p_0 = 0.5, \delta = 1$ (e) $p_0 = 0.5, \delta = 5$ (f) $p_0 = 0.5, \delta = 10$

Figure 4: The effect of p_0 and δ on the final distribution (at the exit) of polarization factor p. Here, $N_R + N_L = 100$ and $I = 0$.

3. Results and Discussion

3.1. Movement without leaders ($I = 0$)

The first set of simulations tries to isolate the effect of initial bias and the effect of varying degree of interactions between evacuees. All simulations were conducted with $N = 100$ without the presence of any strongly opinionated individuals (i.e. $I = 0$). The distribution of final crowd polarization were obtained by running identical experiments 2500 times. The top row in Fig. 4 shows the final distribution of crowd polarization (p) with increasing δ and $p_0 = 0$. The bottom row is for $p_0 = 0.5$, to show the effect of starting with a relatively higher initial polarization. We can interpret that with more interactions amongst the individuals, they end up coalescing completely at either one of the exits (Fig. 4a). If the initial crowd polarization is non zero ($p_0 \neq 0$) then the crowd coalesce more at the exit towards which they are initially biased (Fig. 4d). When the decay rate (δ) is increased, the number of successful interactions goes down and hence the distribution of crowd at the exit become less predictable. The crowd does not get enough chances to successfully interact and coalesce to a unified decision before they reach the exits (Fig. 4c). The initial crowd bias helps to tilt the final distribution towards the respective exit nevertheless. The entire crowd ending up in one of the two exits is generally undesirable unless the state of emergency renders one of the exits unusable.

Figure 5(c) shows the plot of final polarization factor characteristics (mean and entropy) with different strength of interactions. The mean of final polarization factor (in the absence of leaders) depends only on the initial polarization (p_0), but independent of the amount of interactions among nodes. This reinforces the previous argument that the initial crowd bias helps to tilt the final distribution towards the corresponding exit. The entropy is low for lower δ. This conveys that with more interaction the final distribution become more ordered. The entropy goes up with higher δ since the distribution become less predictable. With more initial crowd bias the entropy goes down as the $p_0 \neq 0$ creates a more ordered initial crowd opinion leading to a relative more ordered final crowd opinion. Figures 5(a) and 5(b) show the plots of mean location of the groups moving respectively towards right and left. With lesser interaction the crowd moves quickly towards their respective exit. This is expected since with more interactions among the individuals there is more possibility for them to switch their exit choice midway and thus end up increasing the average number of steps required to reach their desired exit. With a initial biased population towards the right exit ($p_0 > 0$), the average number of steps required by the crowd moving towards the right exit decreases and the average number of steps required by the crowd moving towards left exit increases. Since the initial bias of the crowd reinforces the right opinionated group and conflicts with the left opinionated group, the movement towards the exit in the right side is bolstered and the movement in the opposite direction is impeded. The next sub-section

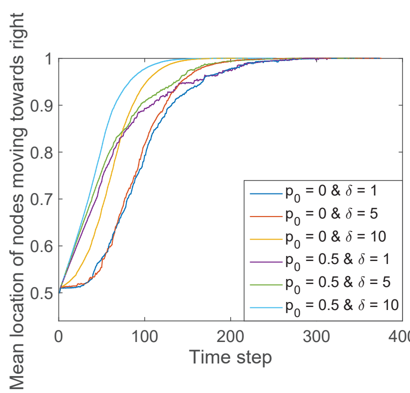

(a)

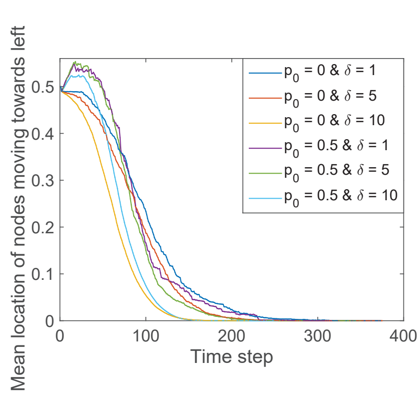

(b)

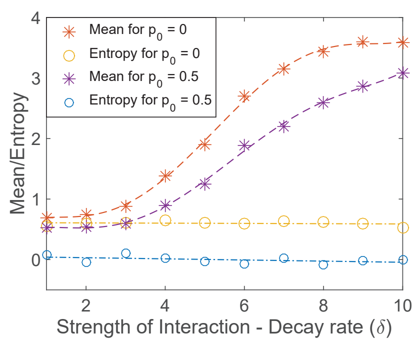

(c)

Figure 5: (a) Movement dynamics for nodes moving towards right exit, (b) Movement dynamics for nodes moving towards left exit and (c) Final polarization factor characteristics with different decay rates and initial polarization factors ($p_0 = 0$ and $p_0 = 0.5$). For all graphs $N_R + N_L = 100$ and $I = 0$.

delves into the dynamics of the crowd in the presence of strong opinion holders ($I > 0$).

3.2. *Movement in the presence of leaders ($I > 0$)*

3.2.1. *Constant u - Variable I*

The next set of experiments were conducted to study the effect of global influence ratio (ζ) during egress. The influencer ratio, i.e $u = (I_R - I_L)/I = -1/11$ is kept constant; initial polarization is maintained at $p_0 = 0$. As in previous section, $N = 100$. Figure 6 shows the distribution of the final polarization of the undecided crowd when varying number of influencing nodes are embedded in the crowd. The distribution was obtained through running the experiment under the same conditions 2500 times. The graphs point out two significant characteristics. With greater magnitude of I, the distribution of polarization factor becomes sharper and shifts towards the side with more number of influencers, in this case towards the left since $I_L > I_R$. With an

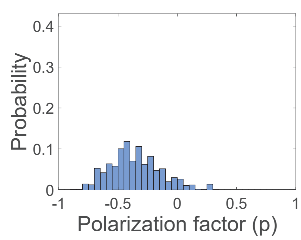

(a) $\zeta = \frac{11}{100}$ ($I_L = 6, I_R = 5$)

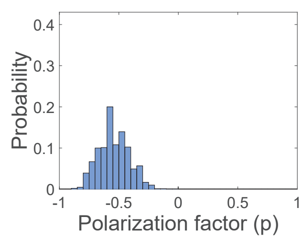

(b) $\zeta = \frac{22}{100}$ ($I_L = 12, I_R = 10$)

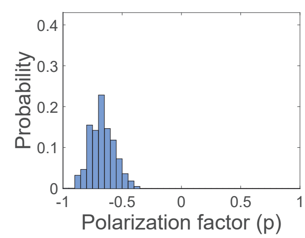

(c) $\zeta = \frac{33}{100}$ ($I_L = 18, I_R = 15$)

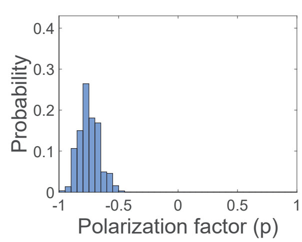

(d) $\zeta = \frac{44}{100}$ ($I_L = 24, I_R = 20$)

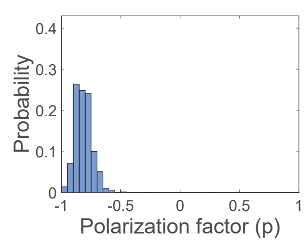

(e) $\zeta = \frac{55}{100}$ ($I_L = 30, I_R = 25$)

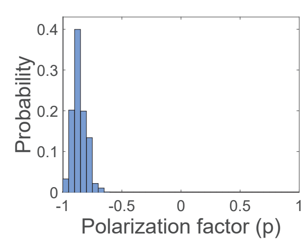

(f) $\zeta = \frac{66}{100}$ ($I_L = 36, I_R = 30$)

Figure 6: Effect of global influence ratio (ζ) with initial polarization $p_0 = 0$, $u = \frac{-1}{11}$, $\delta = 10$ and $N_R + N_L = 100$

increasing global influence ratio, ζ, their reach expands and thus they are able to impact the final outcome with more certainty.

Figure 7(c) displays the mean and entropy of the equilibrium p distribution with varying ζ. The mean shifts towards the side with higher number of influencers and the entropy decreases as the distribution becomes sharper. With more influencers in the crowd, the probability of successful interaction increases since the influencers are not restricted by the distance rule and thus brings down the entropy, i.e. uncertainty in the outcome. The movement dynamics of the crowd is depicted in Figs. 7(a) and

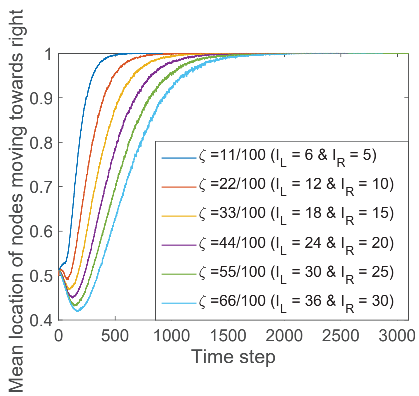

(a)

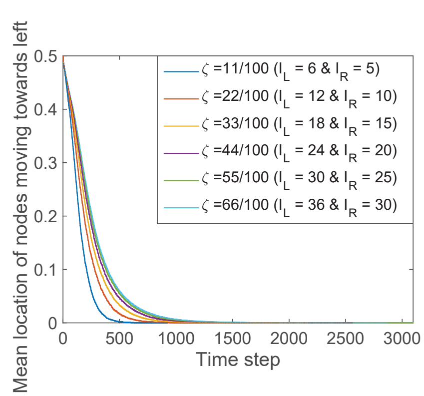

(b)

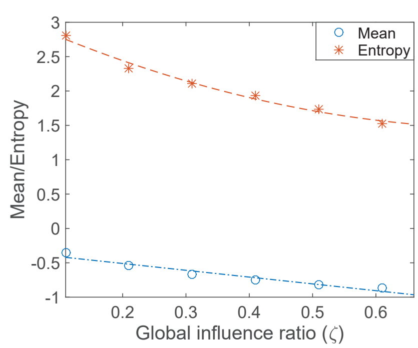

(c)

Figure 7: (a) Movement dynamics for nodes moving towards right exit, (b) Movement dynamics for nodes moving towards left exit and (c) Final crowd polarization characteristics for different ζ. For all graphs $u = \frac{-1}{11}$, $p_0 = 0$, $\delta = 10$ and $N_R + N_L = 100$.

7(b). Since the crowd is attracted to move towards the left exit by a larger number of strongly opinionated individuals, the movement towards the left is quicker compared to the movement towards the opposite side. But, there is a detrimental effect with increasing number of leaders. The average number of steps required by the crowd to reach an exit goes up and this is the effect of a larger number of successful interactions which implies that individuals are more likely to remain indecisive and thus they end up in the corridor for longer period. The next set of experiments were modeled to study the effect of influencer ratio u on the crowd dynamics.

3.2.2. Constant I - Variable u

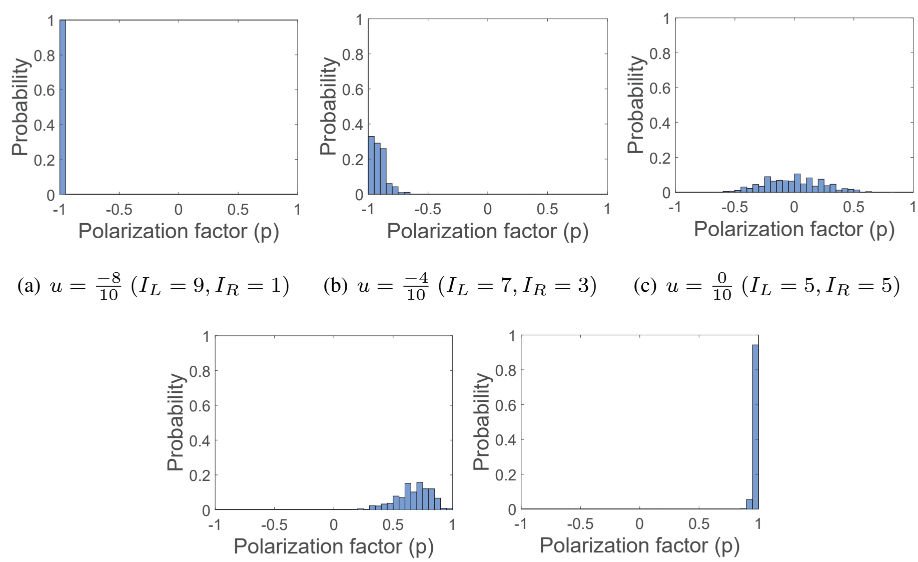

(a) $u = \frac{-8}{10}$ $(I_L = 9, I_R = 1)$ (b) $u = \frac{-4}{10}$ $(I_L = 7, I_R = 3)$ (c) $u = \frac{0}{10}$ $(I_L = 5, I_R = 5)$

(d) $u = \frac{2}{10}$ $(I_L = 4, I_R = 6)$ (e) $u = \frac{6}{10}$ $(I_L = 2, I_R = 8)$

Figure 8: Effect of different influencer ratio (u) with initial polarization $p_0 = 0$, $I = 10$, $\delta = 10$ and $N_R + N_L = 100$

The distribution of the crowd polarization at the exit with $N = 100$, initial condition $p_0 = 0$, $\delta = 10$ and $I = 10$ with different u is illustrated in Fig. 8. As in previous sections, the distribution was obtained by running the simulation 2500 times under same initial conditions. The more skewed the influencer ratio, the higher the probability that the crowd moves en masse towards that particular exit. Even, the presence of strongly opinionated individuals evenly attracting towards both exit, (i.e. $u = 0$) has a desirable effect on the crowd dynamics. The distribution is more condensed than in the case with no influence at all ($I = 0$).

Figure 9(c) presents the mean and entropy of the final polarization factor for different u. The mean has monotonic but non-linear correlation with the influencer ratio (u). The entropy falls as $abs(u)$ increases, since the distributional uncertainty is reduced the more skewed the influence on the population. The influencers ensure that the crowd coalesce more predictably with $u \neq 0$. Figure 9(a) depicts the movement dynamics of the crowd moving toward the exit on the right side for $u > 0$. With increasing u from

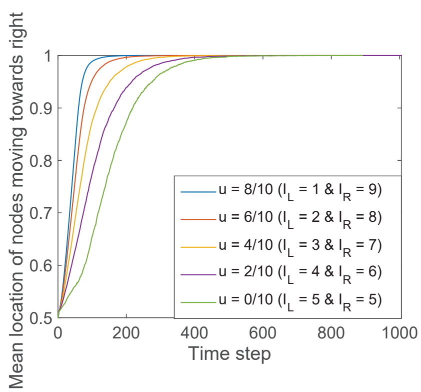

(a)

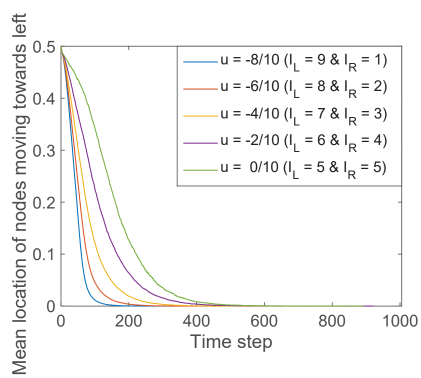

(b)

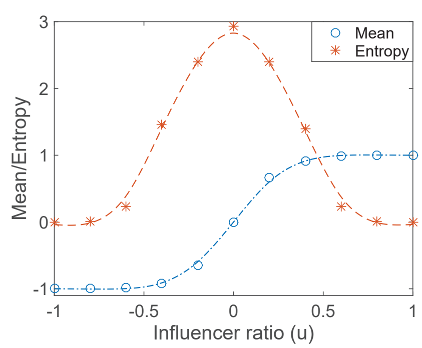

(c)

Figure 9: (a) Movement dynamics for nodes moving towards right exit, (b) Movement dynamics for nodes moving towards left exit and (c) Final crowd polarization characteristics for different u. Here, $p_0 = 0$, $I = 10$, $\delta = 10$ and $N_R + N_L = 100$.

0 to 1 the movement towards the right side exit becomes quicker since the influencers attract the crowd towards the right side exit more strongly. Figure 9(b) portrays the movement of crowd which movers towards the exit on the left side of the corridor for $u < 0$. With decreasing u from 0 to -1, the average number of steps required by the crowd to egress through the left side exit goes down. The influencers are able to shepherd the crowd more effectively towards the left side exit with decreasing u. Thus it can be concluded that with lesser total number of strong opinion holder (I) and $u \neq 0$, the crowd can be split into any ratio for optimally utilizing the exits and thus achieve quicker evacuation of the crowd from the hazardous situation.

3.2.3. Constant u *and* I *- Variable* p_0 *and* δ

The last set of experiments were conducted to study the effect of different initial bias (p_0) and decay rate of communication (δ) with constant numbers of strongly opinionated individuals ($I_L = 5$ and $I_R = 2$) amongst the crowd ($N = 100$). Figure 10(a) brings out the characteristics of final crowd polarization factor with different initial crowd polarization (p_0) and decay rates (δ). With a small number of strong opinion holders, the mean of the final polarization factor is only slightly affected by the initial crowd bias for different strength of interaction and different initial crowd polarization. This leads to the conclusion that with a relatively few strong opinion holders the crowd can be directed such that they end up utilizing the exits optimally.

Figure 10(b) shows the effect of strength of interaction on the final polarization factor characteristics. With lesser interactions, the effect of strong opinion holders on the mean diminishes slightly. This is because individuals other than the influencers have lesser probability of successful interactions and thus the secondary passing of influencers' opinions is restricted with increasing δ. From an information content point of view, the entropy decreases when the initial crowd bias (p_0) favors the influencer ratio ($p_0 < 0$ and $u < 0$ or $p_0 > 0$ and $u > 0$). Since the initial crowd polarization and influencer ratios reinforce one another the uncertainty and consequently the entropy goes down. When the initial crowd polarization opposes the influencer ratio ($p_0 < 0$ and $u > 0$ or $p_0 > 0$ and $u < 0$), the entropy increases. The entropy increases with increasing δ. With lesser probability of successful interaction, the effect of influencer

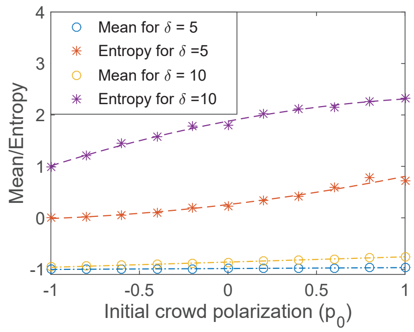

(a)

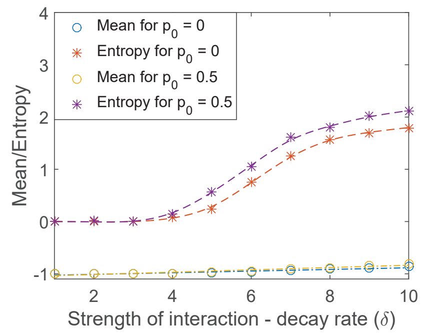

(b)

Figure 10: Final crowd polarization characteristics (a) For different p_0 and (b) For different δ. $N_R + N_L = 100$.

propagate more slowly and hence the increase in entropy with increasing δ.

4. Conclusion

This work is unique in the sense it combines a motion model with a explicit opinion sharing model to study the effects of opinion sharing on crowd evacuation from a long corridor with exits at each end. People with leadership skills and strong bias towards a particular exit play a pivotal role in determining how the crowd is dynamically attracted towards each of the exits. The effect of leaders on the dynamics of the hybrid model is studied in detail.

In contrast to existing models, which usually focuses more on developing realistic motion models, this work tries to combine the effect of opinion sharing and movement among egressing individuals and also discusses interesting effects of strongly opinionated leaders in shaping the crowd movement dynamics. Also, different strengths of interaction were tested and an analytical solution for a interaction zone restricted interaction were presented.

References

[1] R. Hughes, The flow of large crowds of pedestrians, Mathematics and Computers in Simulation 53 (4) (2000) 367–370.

[2] R. L. Hughes, A continuum theory for the flow of pedestrians, Transportation Research Part B: Methodological 36 (6) (2002) 507–535.

[3] R. L. Hughes, The flow of human crowds, Annual review of fluid mechanics 35 (1) (2003) 169–182.

[4] R. M. Colombo, M. D. Rosini, Pedestrian flows and non-classical shocks, Mathematical Methods in the Applied Sciences 28 (13) (2005) 1553–1567.

[5] J. Dijkstra, H. J. Timmermans, A. Jessurun, A multi-agent cellular automata system for visualising simulated pedestrian activity, in: Theory and Practical Issues on Cellular Automata, Springer, 2001, pp. 29–36.

[6] D. Helbing, P. Molnar, Social force model for pedestrian dynamics, Physical review E 51 (5) (1995) 4282.

[7] D. Helbing, Traffic and related self-driven many-particle systems, Reviews of modern physics 73 (4) (2001) 1067.

[8] C. Burstedde, K. Klauck, A. Schadschneider, J. Zittartz, Simulation of pedestrian dynamics using a two-dimensional cellular automaton, Physica A: Statistical Mechanics and its Applications 295 (3) (2001) 507–525.

[9] A. Varas, M. Cornejo, D. Mainemer, B. Toledo, J. Rogan, V. Munoz, J. Valdivia, Cellular automaton model for evacuation process with obstacles, Physica A: Statistical Mechanics and its Applications 382 (2) (2007) 631–642.

[10] M. Seitz, G. Köster, A. Pfaffinger, Pedestrian group behavior in a cellular automaton, in: Pedestrian and Evacuation Dynamics 2012, Springer, 2014, pp. 807–814.

[11] A. Kirchner, H. Klüpfel, K. Nishinari, A. Schadschneider, M. Schreckenberg, Simulation of competitive egress behavior: comparison with aircraft evacuation data, Physica A: Statistical Mechanics and its Applications 324 (3) (2003) 689–697.

[12] A. Kirchner, A. Schadschneider, Simulation of evacuation processes using a bionics-inspired cellular automaton model for pedestrian dynamics, Physica A: Statistical Mechanics and its Applications 312 (1) (2002) 260–276.

[13] A. Kirchner, H. Klüpfel, K. Nishinari, A. Schadschneider, M. Schreckenberg, Discretization effects and the influence of walking speed in cellular automata models for pedestrian dynamics, Journal of Statistical Mechanics: Theory and Experiment 2004 (10) (2004) P10011.

[14] H. L. Kluepfel, A cellular automaton model for crowd movement and egress simulation, Ph.D. thesis, Universität Duisburg-Essen, Fakultät für Physik (2003).

[15] C. M. Henein, T. White, Macroscopic effects of microscopic forces between agents in crowd models, Physica A: statistical mechanics and its applications 373 (2007) 694–712.

[16] D. Parisi, C. Dorso, Microscopic dynamics of pedestrian evacuation, Physica A: Statistical Mechanics and its Applications 354 (2005) 606–618.

[17] D. R. Parisi, C. O. Dorso, Morphological and dynamical aspects of the room evacuation process, Physica A: Statistical Mechanics and its Applications 385 (1) (2007) 343–355.

[18] D. Helbing, M. Isobe, T. Nagatani, K. Takimoto, Lattice gas simulation of experimentally studied evacuation dynamics, Physical review E 67 (6) (2003) 067101.

[19] K. Takimoto, T. Nagatani, Spatio-temporal distribution of escape time in evacuation process, Physica A: Statistical Mechanics and its Applications 320 (2003) 611–621.

[20] W. Song, X. Xu, B.-H. Wang, S. Ni, Simulation of evacuation processes using a multi-grid model for pedestrian dynamics, Physica A: Statistical Mechanics and its Applications 363 (2) (2006) 492–500.

[21] R. Guo, H.-J. Huang, A mobile lattice gas model for simulating pedestrian evacuation, Physica A: Statistical Mechanics and its Applications 387 (2) (2008) 580–586.

[22] P. Lino, G. Maione, B. Maione, Modeling and simulation of crowd egress dynamics in a discrete event environment, in: Control Applications,(CCA) & Intelligent Control,(ISIC), 2009 IEEE, IEEE, 2009, pp. 843–848.

[23] H. Singh, R. Arter, L. Dodd, P. Langston, E. Lester, J. Drury, Modelling subgroup behaviour in crowd dynamics dem simulation, Applied Mathematical Modelling 33 (12) (2009) 4408–4423.

[24] S. M. Lo, H.-C. Huang, P. Wang, K. Yuen, A game theory based exit selection model for evacuation, Fire Safety Journal 41 (5) (2006) 364–369.

[25] Y. Gao, P. B. Luh, Q. Zhao, H. Zhang, N. Wu, L. Qiao, Fire evacuation model with confidence intervals, in: Automation Science and Engineering (CASE), 2011 IEEE Conference on, IEEE, 2011, pp. 731–736.

[26] P. Wang, P. B. Luh, S.-C. Chang, J. Sun, Modeling and optimization of crowd guidance for building emergency evacuation, in: Automation Science and Engineering, 2008. CASE 2008. IEEE International Conference on, IEEE, 2008, pp. 328–334.

[27] G. Proulx, Understanding human behaviour in stressful situations (2002).

[28] S. Hasan, S. V. Ukkusuri, Social contagion process in informal warning networks to understand evacuation timing behavior, Journal of Public Health Management and Practice 19 (2013) S68–S69.

[29] R. L. Goldstone, M. A. Janssen, Computational models of collective behavior, Trends in cognitive sciences 9 (9) (2005) 424–430.

[30] K. Bergey, K. Spieser, D. E. Davison, The psychological dynamics of students in a classroom: Modeling and control strategies based on suggestibility theory, in: Control Applications, 2007. CCA 2007. IEEE International Conference on, IEEE, 2007, pp. 658–663.

[31] K. Spieser, D. Davison, Stabilizing the psychological dynamics of people in a queue, in: American Control Conference, 2008, IEEE, 2008, pp. 4173–4178.

[32] K. Spieser, D. E. Davison, Multi-agent stabilisation of the psychological dynamics of one-dimensional crowds, Automatica 45 (3) (2009) 657–664.

[33] K. Spieser, Stabilizing the psychological dynamics of people in a crowd, Ph.D. thesis, University of Waterloo (2008).

[34] G. Le Bon, The crowd: A study of the popular mind, Fischer, 1897.

[35] X. Pan, C. Han, K. H. Law, J.-C. Latombe, A computational framework to simulate human and social behaviors for egress analysis, in: Proceedings of the Joint International Conference on Computing and Decision Making in Civil and Building Engineering, 2006, pp. 1206–1215.

[36] X. Pan, Computational modeling of human and social behaviors for emergency egress analysis, Ph.D. thesis, Stanford University (2006).

[37] X. Pan, C. S. Han, K. Dauber, K. H. Law, A multi-agent based framework for the simulation of human and social behaviors during emergency evacuations, Ai & Society 22 (2) (2007) 113–132.

[38] M. L. Chu, X. Pan, K. Law, Incorporating social behaviors in egress simulation, in: Proceedings of 2011 Computing in Civil Engineering Workshop, 2011, pp. 19–22.

[39] E. Kuligowski, Review of 28 egress models, NIST SP 1032.

[40] X. Zheng, T. Zhong, M. Liu, Modeling crowd evacuation of a building based on seven methodological approaches, Building and Environment 44 (3) (2009) 437–445.

[41] S. Chakraborty, Analytical methods to investigate the effects of external influence on socio-cultural opinion evolution, in: Social Computing, Behavioral-Cultural Modeling and Prediction, Springer, 2013, pp. 386–393.

[42] A. R. Srinivasan, S. Chakraborty, Effect of network topology on the controllability of voter model dynamics using biased nodes, in: American Control Conference (ACC), 2014, IEEE, 2014, pp. 2096–2101.

[43] E. Wong, J. Thomas, On polynomial expansions of second-order distributions, Journal of the Society for Industrial and Applied Mathematics 10 (3) (1962) 507–516.